DNA Repair 12 (2013) 196–204

Contents lists available at SciVerse ScienceDirect

DNA Repair

journal homepage: www.elsevier.com/locate/dnarepair

Non-productive DNA damage binding by DNA glycosylase-like protein Mag2 from *Schizosaccharomyces pombe*☆

Suraj Adhikary, Marilyn C. Cato, Kriston L. McGary, Antonis Rokas, Brandt F. Eichman*

Department of Biological Sciences, Vanderbilt University, Nashville, TN 37232, United States

ARTICLE INFO

Article history:
Received 7 November 2012
Received in revised form 3 December 2012
Accepted 3 December 2012
Available online 28 December 2012

Keywords:
Base excision repair
DNA glycosylase
Ethenoadenine
3-Methyladenine
Protein–DNA interactions

ABSTRACT

Schizosaccharomyces pombe contains two paralogous proteins, Mag1 and Mag2, related to the helix-hairpin-helix (HhH) superfamily of alkylpurine DNA glycosylases from yeast and bacteria. Phylogenetic analysis of related proteins from four *Schizosaccharomyces* and other fungal species shows that the Mag1/Mag2 duplication is unique to the genus *Schizosaccharomyces* and most likely occurred in its ancestor. Mag1 excises *N*3- and *N*7-alkylguanines and 1,N^6-ethenoadenine from DNA, whereas Mag2 has been reported to have no detectible alkylpurine base excision activity despite high sequence and active site similarity to Mag1. To understand this discrepancy we determined the crystal structure of Mag2 bound to abasic DNA and compared it to our previously determined Mag1–DNA structure. In contrast to Mag1, Mag2 does not flip the abasic moiety into the active site or stabilize the DNA strand 5′ to the lesion, suggesting that it is incapable of forming a catalytically competent protein–DNA complex. Subtle differences in Mag1 and Mag2 interactions with the DNA duplex illustrate how Mag2 can stall at damage sites without fully engaging the lesion. We tested our structural predictions by mutational analysis of base excision and found a single amino acid responsible at least in part for Mag2's lack of activity. Substitution of Mag2 Asp56, which caps the helix at the base of the DNA intercalation loop, with the corresponding serine residue in Mag1 endows Mag2 with εA excision activity comparable to Mag1. This work provides novel insight into the chemical and physical determinants by which the HhH glycosylases engage DNA in a catalytically productive manner.

1. Introduction

All organisms are equipped with a number of DNA glycosylases that initiate base excision repair (BER) of potentially harmful alkylated, oxidized, and deaminated nucleobases from DNA [1]. Upon locating an aberrant nucleotide, DNA glycosylases catalyze hydrolysis of the *N*-glycosidic bond to produce an abasic site, which is subsequently processed by an apurinic/apyrimidinic (AP) endonuclease, DNA polymerase, and DNA ligase activities to fully repair the damage [1]. In order to break the *N*-glycosidic bond, DNA glycosylases trap the damaged nucleotide in an extrahelical conformation in which the nucleobase is pulled out of the DNA base stack and tucked into the enzyme's active site. The extruded DNA is stabilized by several side chains that intercalate into the base stack at the damage site. The importance of these stabilizing interactions to catalysis is underscored by the fact that mutation of the intercalating residues renders the glycosylase inactive [2–6], and recent work illustrates how they may play an active role in detecting or even discriminating against certain types of damage [7–10].

DNA glycosylases specialized for alkylation damage are found in all organisms. The mammalian AAG enzyme is structurally unique and removes a variety of modified purines, including *N*3-methyladenine (3mA), *N*7-methylguanine (7mG), 1,N^6-ethenoadenine (εA), as well as hypoxanthine, a deamination product of adenine [11–16]. The bacterial (TAG, AlkA) and yeast (Mag, Mag1) enzymes all belong to the helix-hairpin-helix (HhH) structural superfamily and exhibit a range of substrate specificities [1]. TAG is constitutively active and highly specific for 3mA and 3mG, whereas AlkA is induced as part of the adaptive response to alkylation exposure and shares AAG's broad substrate preference [1,17]. Similar to AlkA, *Saccharomyces cerevisiae* Mag is inducible, lacks specificity for any particular alkylpurine, and exhibits a strong mutator phenotype [18–21].

The genetically tractable fission yeast, *Schizosaccharomyces pombe*, has provided a convenient model system to investigate

Abbreviations: 3mA, *N*3-methyladenine; 7mG, *N*7-methylguanine; εA, 1,N^6-ethenoadenine; Mag, yeast 3-methyladenine DNA glycosylase; TAG, bacterial 3-methyladenine DNA glycosylase I; AlkA, bacterial 3-methyladenine DNA glycosylase II; AAG, mammalian alkyladenine DNA glycosylase.

☆ *Database*: PDB 4HSB.

* Corresponding author at: 465 21st Avenue South, MRBIII 5270A, Nashville, TN 37232, United States. Tel.: +1 615 936 5233; fax: +1 615 936 2211.
E-mail address: brandt.eichman@vanderbilt.edu (B.F. Eichman).

1568-7864/$ – see front matter © 2012 Elsevier B.V. All rights reserved.
http://dx.doi.org/10.1016/j.dnarep.2012.12.001

the importance of individual components to BER [22]. *S. pombe* contains one alkylpurine glycosylase, Mag1, which removes 3mA, 7mG, and εA at lower rates than Mag, partially explaining why Mag1 is not as critical to alkylation resistance as Mag and AlkA [10,21,23–25]. The crystal structure of Mag1 in complex with abasic DNA revealed a unique protein–DNA contact that inhibited activity toward εA, partially explaining the difference in activity with Mag [10]. *S. pombe* contains a related protein, Mag2, which shares 41% sequence identity and 69% overall similarity to Mag1, but lacks glycosylase activity [25]. Genetic studies with *S. pombe* strains *mag1*Δ and *mag2*Δ showed no increase in alkylation sensitivity, whereas *nth1*Δ (AP lyase), *apn2*Δ (AP endonuclease) and *rad2*Δ (flap endonuclease) are all sensitive to MMS [25]. Interestingly, strains harboring double deletions in *nth1*Δ *mag1*Δ, *nth1*Δ *mag2*Δ, *apn2*Δ *mag1*Δ, and *rad2*Δ *mag1*Δ restored MMS resistance [24–26], indicating that Mag1 is involved in BER and that Mag2 may play a role in Nth1-mediated DNA repair, although alkylation damage may not be the preferred substrate of either enzyme. These studies also showed that exogenous expression of either Mag1 or Mag2 in a *rad16*Δ/*mag1*Δ/*mag2*Δ triple mutant restores MMS resistance lost as a result of the deletions [26]. However, the lack of glycosylase activity of Mag2 *in vitro* has made it difficult to understand its role and the need for two highly homologous enzymes in *S. pombe*.

In order to understand the lack of base excision activity by Mag2, we carried out an evolutionary analysis of Mag-related genes in yeasts and related fungi and determined the crystal structure of Mag2 in complex with DNA containing an abasic site. We find that duplication of Mag1 and Mag2 is specific to the *Schizosaccharomyces* clade, suggesting that the two proteins diverged at least 200 million years ago [27], and that *S. pombe* Mag2 experienced an accelerated rate of evolution relative to Mag1. Interestingly, the Mag2 structure shows that unlike Mag1, the abasic site is not extruded in the active site and the DNA 5′ to the lesion is disordered, suggesting that the lack of activity is a consequence of the inability of Mag2 to engage the substrate. Comparison of Mag1 and Mag2 DNA complexes illuminates structural features necessary for DNA damage recognition by this family of DNA glycosylases. We show by mutagenesis that inhibition of Mag2 base excision activity can be explained by a negatively charged, helix-capping interaction at the base of the structural motif that normally stabilizes the extrahelical nucleotide, which further underscores the importance of DNA intercalating residues to base excision activity.

2. Materials and methods

2.1. Evolutionary analysis

The amino acid sequences of *S. cerevisiae* Mag and *S. pombe* Mag1 and Mag2 were used to query a fungal BLAST database containing more than 200 fungal genomes, as previously described [28]. A preliminary neighbor joining tree constructed using the full sequences of the BLAST hits revealed that the Mag1/2 paralogs only occur in the *Schizosaccharomyces* clade, and that only a single Mag homolog exists in most other fungi. To accurately infer the evolutionary history of the Mag1/Mag2 duplication, an automated alignment was constructed from Mag1/Mag2 homologs in representative fungal species using MAFFT v6.952b [29] with settings recommended for high accuracy (maxiterate = 1000 and localpair). The Mag1/Mag2 phylogeny was constructed from the alignment using the maximum likelihood optimality criterion as implemented in RAxML 7.2.6 [30]. The phylogenetic analysis was performed using the PROTGAMMALGF model, which had the best fit to the alignment data according to the ProteinModelSelection.pl test, packaged with RAxML. Robustness in phylogeny inference was assessed with 1000 bootstrap replicates and plotted on the maximum likelihood phylogeny.

2.2. Protein purification

The Mag2 gene was PCR amplified from *S. pombe* genomic DNA and cloned into pBG100 (Vanderbilt Center for Structural Biology) to produce an N-terminal His_6-tagged protein. Protein was overexpressed in *E. coli* BL21 cells for 16 h at 16 °C upon addition of 0.5 mM IPTG. Cells were lysed in 50 mM Tris–HCl (pH 8.0), 500 mM NaCl, and 10% glycerol and protein isolated using Ni-NTA (Qiagen) affinity chromatography. Following cleavage of the His_6 tag by Rhinovirus 3C (PreScission) protease overnight, Mag2 was purified by anion-exchange (HiTrap Q-HP, GE Healthcare) chromatography in buffer A (20 mM Tris–HCl (pH 8.0), 1 mM DTT and 0.05 mM EDTA) using a 0–1 M NaCl linear gradient, followed by gel filtration (Superdex 200, GE Healthcare) in buffer A/150 mM NaCl. The Mag2 Asp56Ser mutant was generated using a Quik-Change kit (Stratagene) and purified the same as wild-type.

2.3. X-ray crystallography

Protein–DNA complexes were assembled by incubating 0.30 mM Mag2 with 0.36 mM DNA (d(CGGACT (THF)ACGGG)/d(GCCCGTTAGTCC) at 4 °C for 20 min. Crystals were grown by vapor diffusion at 21 °C against reservoir solution containing 50 mM NaHEPES (pH 7.5), 50% PEG 200, 200 mM KCl and 25 mM $MgSO_4$. Crystals were flash frozen in mother liquor containing 60% PEG 200 prior to data collection. X-ray diffraction data (Supplementary Information) to 1.9 Å were collected at the 21-ID-F beamline at the Advanced Photon Source (Argonne, IL) and processed using HKL2000 [31]. Phases were determined by molecular replacement using the protein structure of *S. pombe* Mag1 from PDB ID 3S6I as a search model. Simulated annealing and restrained coordinate refinement [32] improved the quality of the maps and allowed visualization of the DNA, with the exception of nucleotides (C1-T6) on the damaged strand the 5′-overhang (G1) on the opposite strand. DNA atoms were built using COOT [33] and the model refined against 1.9 Å diffraction data using a maximum likelihood target in PHENIX [34]. At this stage nucleotides G2–G3 and phosphates for A4–T6 were visible in 2Fo-Fc and Fo-Fc electron density maps, which allowed construction of the remaining nucleotides on the 5′-end of the damaged strand. Iterative coordinate and B-factor refinement and model building were carried out in PHENIX and COOT. Anisotropic motion of different protein/DNA fragments were modeled using translation/libration/screw-rotation (TLS) refinement. Individual anisotropic B-factors derived from the refined TLS parameters were held fixed during subsequent rounds of refinement. The final model, consisting of amino acids 5–209 and nucleotides 2–12 and one protein/DNA complex in the asymmetric unit, was validated using PROCHECK [35]. 94.1% and 5.9% of protein residues reside in allowed and additional allowed regions of the Ramachandran plot, respectively, and no residues reside in generously allowed or disallowed regions. The N9—C1′—O4′ (G2) and C3′—C4′—O4′ (G3) bond angles for nucleotides G2 and G3 on the disordered portion of the damaged strand deviated more than 6 times the standard deviation from ideal values. Nucleic acid parameters were calculated using CURVES [36]. The final model was deposited in the Protein Data Bank under accession number 4HSB.

2.4. Base excision activity

Base excision activity was measured as described for Mag1 [10]. Unmodified and εA-containing oligonucleotides were purchased from Integrated DNA Technologies. The sequence tested was

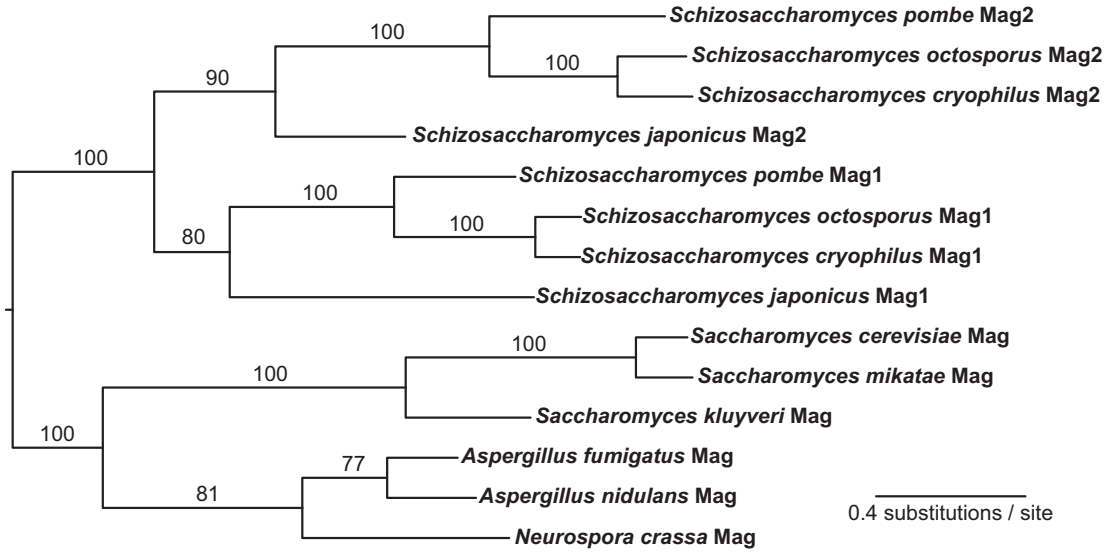

Fig. 1. Phylogenetic history of the Mag family of proteins from *Schizosaccharomyces* and representative fungal relatives. Numbers above branches represent bootstrap support and branch lengths represent protein evolutionary rate in units of amino acid substitutions per site. The Mag phylogeny shows that the duplication of Mag1 and Mag2 is specific and unique to the *Schizosaccharomyces* clade and that both paralogs have been retained in all 4 *Schizosaccharomyces* species.

d(GACCACTACACC(εA)TTTCCTAACAAC)/d(GTTGTTAGGAAATGGT-GTAGTGGTC). Reactions were carried out at 25 °C, 120 mM ionic strength, and pH 6.0. Reactions were terminated at various times with 0.2 M NaOH and heated at 70 °C for 2 min. Substrate and NaOH-cleaved product DNAs were separated on 15% polyacrylamide/7 M urea gel and quantified by autoradiography. Experiments were performed in triplicate.

3. Results

3.1. Evolutionary analysis reveals that Mag1 and Mag2 were duplicated in the ancestor of the Schizosaccharomyces clade and preserved

BLAST analysis of Mag-related proteins across fungi finds a single high scoring homolog of Mag in most fungal genomes. An evolutionary analysis reveals that the duplication of Mag1 and Mag2 is specific to the *Schizosaccharomyces* clade with both paralogs retained in all 4 *Schizosaccharomyces* species with sequenced genomes (*S. pombe*, *Schizosaccharomyces octosporus*, *Schizosaccharomyces cryophilus*, and *Schizosaccharomyces japonicus*). As seen in Fig. 1, after duplication, the topology of the tree matches the established phylogenetic relationships of the species. Given that the divergence of the 4 *Schizosaccharomyces* species is estimated to have taken place approximately 200 million years ago [27], the long-term preservation of both paralogs in all four species suggests that purifying selection is maintaining both copies. The phylogenetic tree also reveals that the lineage leading to *S. pombe* Mag2 experienced an accelerated rate of amino acid substitutions relative to Mag1, which suggests that it has diverged further from Mag's ancestral function than Mag1.

3.2. Mag2 is not an alkylpurine DNA glycosylase

The reported lack of base excision activity by Mag2 is surprising given the sequence conservation to Mag1 in residues that we had previously identified as the Mag1 active site. We therefore tested εA excision activity of Mag2 under conditions that support Mag1 εA activity. Using a standard assay involving alkaline hydrolysis of abasic sites generated by glycosylase action, we were unable to detect significant excision of εA at enzyme concentrations as high as 10 μM and reaction times of 48 h (Fig. 4). Since all Mag orthologs tested show at least low levels of activity for εA [10], our results are consistent with Mag2 being deficient as an alkylpurine DNA glycosylase.

3.3. Structure of the Mag2–DNA complex

To glean structural insight into the lack of base excision activity, we crystallized Mag2 in complex with DNA containing a centrally located tetrahydrofuran (THF) abasic site analog on one strand. We used this same strategy previously to determine the structure of a Mag1/THF–DNA complex since THF closely mimics the structural properties of natural abasic sites but is refractory to hydrolysis [37]. In cases where both substrate and product complexes have been crystallized, the conformation of the abasic-DNA is remarkably similar to that of the substrate, consistent with the fact that glycosylases typically display high affinities for the abasic-DNA product [38] [21,39–41]. The Mag2–DNA crystal structure was determined by molecular replacement using the Mag1 protein as a search model. A crystallographic model with one Mag2–DNA complex in the asymmetric unit was refined against 1.9 Å native diffraction data to a crystallographic residual of 19.2% (R_{free} = 23.5%) (Table S1).

The structure confirmed that Mag2 adopts the HhH architecture common to yeast Mag/Mag1 and bacterial TAG/AlkA. Mag2 consists of two α-helical subdomains—one spanning helices C–J that contains the HhH DNA binding motif (helices I–J) and a second containing the N- and C-termini (helices A–B and K–M) (Fig. 2A). The HhH domain anchors the protein to the DNA through three similar helix-coil-helix interactions—helices CD, which contains the DNA interrogation loop, FG, and IJ, which forms the HhH motif (Fig. 2). The protein binds both strands of the DNA primarily through electrostatic interactions with the phosphate backbone, with the majority of protein–DNA contacts formed between the HhH motif and the 3′ half of the damaged strand (Fig. 2B). As a consequence, the abasic site is directed across the deep cavity at the interface between the two subdomains, which normally forms the active site/nucleobase binding pocket (Fig. 2A). There is a 70° bend in the DNA toward the major groove as a result of Leu54 at the tip of the helix C–D loop wedging itself into the duplex on the undamaged strand. This general mode of DNA binding is the same as that

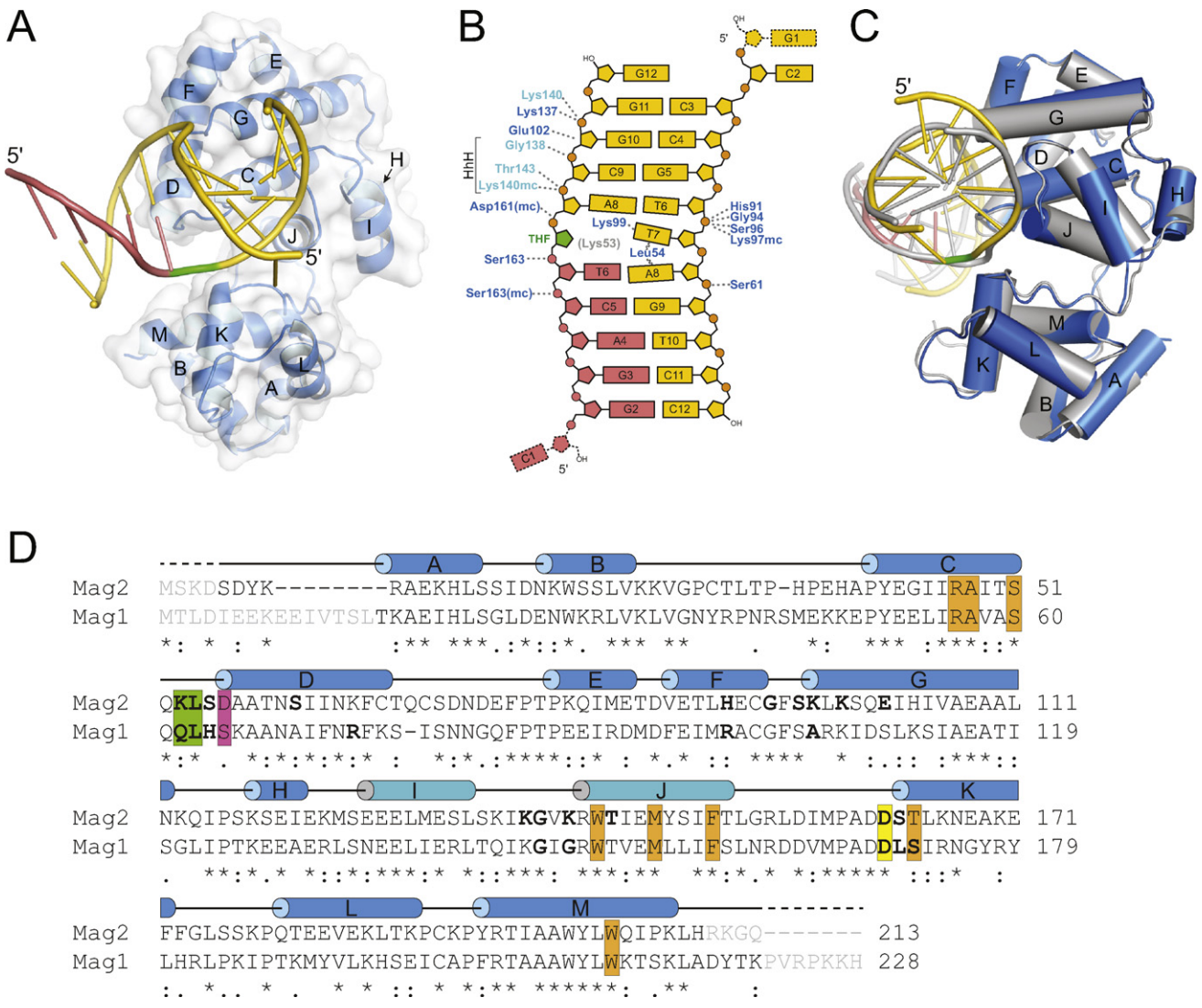

Fig. 2. Crystal structure of *S. pombe* Mag2 bound to abasic-DNA. (A) Mag2 (blue ribbons, white solvent accessible surface) in complex with DNA (gold) containing a THF abasic site analog (green). The disordered stretch of DNA is colored salmon. (B) Schematic of Mag2–DNA interactions, colored as in panel A with HhH residues in cyan. Dotted lines represent either hydrogen bonds or van der Waals interactions. *mc*, main chain. (C) Superposition of Mag2/THF–DNA (colored as in panel A) onto *S. pombe* Mag1/THF–DNA (PDB ID 3S6I, silver). (D) Structure based sequence alignment of Mag1 and Mag2, generated with Swiss PDB Viewer [51]. Secondary structure elements are shown above the alignment. The HhH loop is represented as light blue cylinders. Nucleobase binding pocket residues are highlighted orange, intercalating plug and wedge residues are green, and the catalytic aspartate found in HhH glycosylases is yellow. Mag2 Asp56, responsible for diminished base excision activity, is highlighted magenta. Residues involved in protein-DNA interactions are in bold. (For interpretation of the references to color in this figure legend, the reader is referred to the web version of the article.)

seen in the Mag1/THF–DNA structure. The structures of Mag1 and Mag2 are virtually identical, with an r.m.s.d. of 1.30 Å for all protein backbone atoms (Fig. 2C). The positions of side chains forming the nucleobase binding pocket in Mag1 are all conserved in Mag2, as expected from the sequence identity in these residues (Fig. 2D).

3.4. A partially bound enzyme–DNA complex

In the structure of Mag1 in complex with THF–DNA, the THF moiety was flipped toward the nucleobase binding pocket, and the gap in the duplex stabilized by the Gln62 side chain. Surprisingly, in Mag2 the THF remains stacked into the duplex (Fig. 3A and B), despite the fact that the residues in the nucleobase binding pocket are identical between the two proteins. The electron density clearly supports this un-flipped conformation, with no discernible density in the location of the THF in the Mag1 structure (Supplementary Figure S1). Consequently, the side chain for Lys53, which corresponds to the intercalating Gln62 plug residue in Mag1, is disordered (Fig. 3A). In addition, the entire strand to the 5′-side of the lesion is disordered, as evident from the significantly higher B-factors for those nucleotides (Fig. 3C). Interestingly, the 5′-side of the damaged strands in other HhH structures is generally well-ordered despite any significant protein–DNA contacts in that region of the duplex. We can rule out crystal packing as the reason for the disorder in the Mag2 DNA because the ends of the DNA are base stacked against a symmetry mate, and the B-factors for the stacking residue G2 are lower than its neighbors (Fig. 3C). Thus, unlike other DNA glycosylases, Mag2 does not flip an abasic site toward the conserved nucleobase binding pocket and does not fully engage the DNA duplex on one side of the lesion.

3.5. A structural basis for the lack of glycosylase activity in Mag2

The conservation of the nucleobase binding pocket and bulky intercalating residues (Lys53 and Leu54) would seemingly all favor a flipped conformation of the DNA. Why, then, does Mag2 not engage the abasic site? We reasoned that the answer lies in the subtle differences at the protein–lesion interfaces of Mag1 and Mag2.

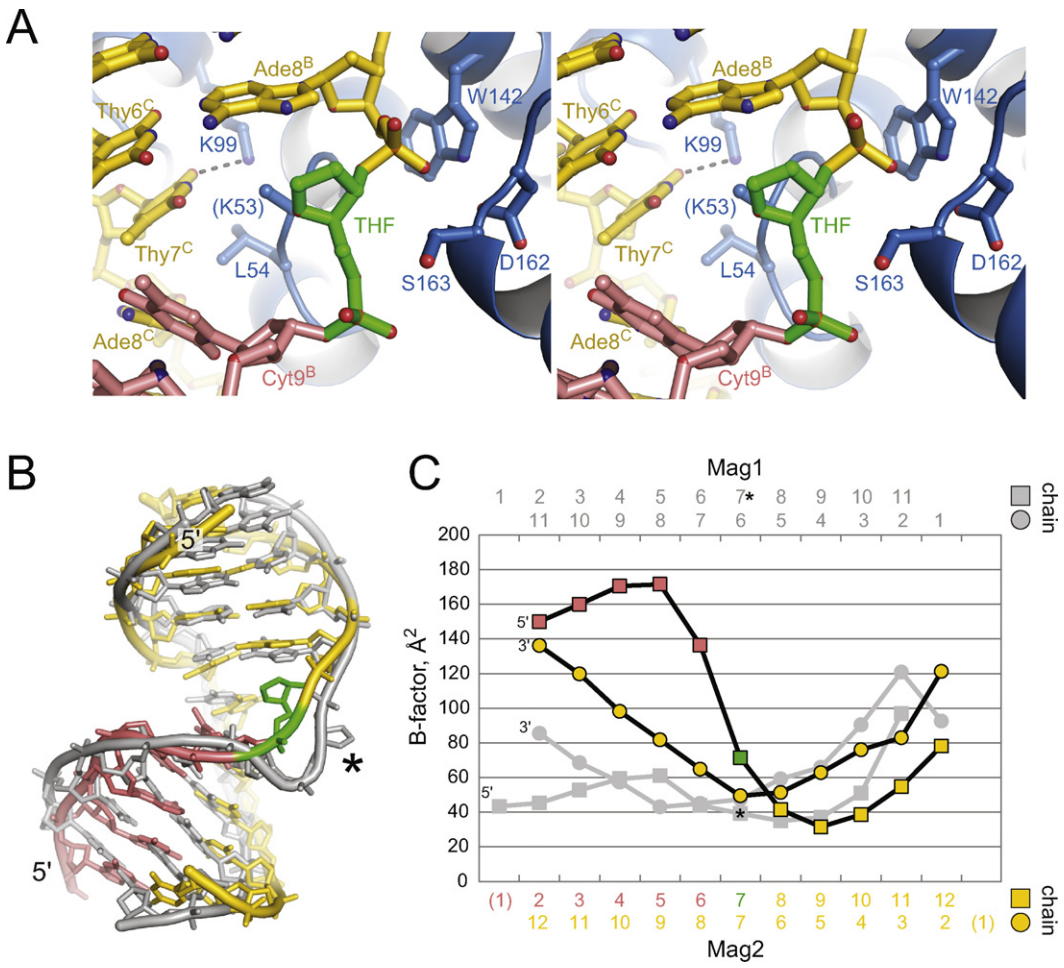

Fig. 3. Mag2 does not flip abasic sites. (A) Stereoview of the region around the THF abasic site in Mag2. Protein and DNA are colored by carbon atom as in Fig. 2. (B) Superposition of DNA bound to Mag1 (gray) and Mag2 (gold/green/salmon). The THF moiety is flipped out of the duplex in the Mag1 structure (denoted with an asterisk) but remains stacked in the duplex in the Mag2 structure (green). (C) Average B-factor per nucleotide between Mag2 (gold/green/salmon) and Mag1 (gray) complexes. The THF-containing and unmodified strands are shown as squares and circles, respectively. (For interpretation of the references to color in this figure legend, the reader is referred to the web version of the article.)

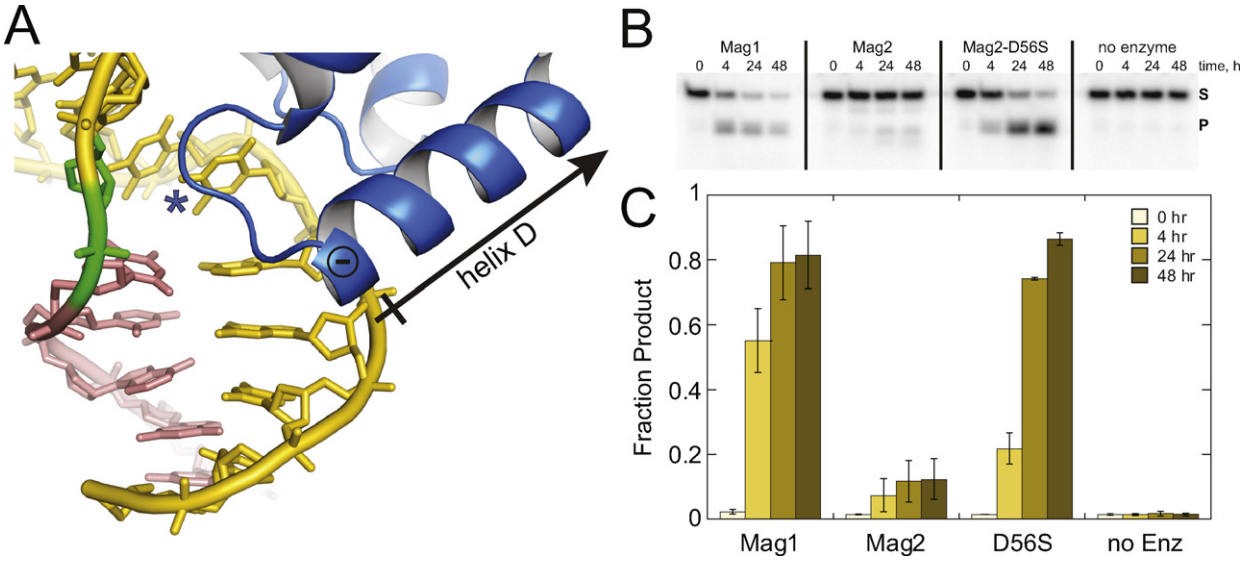

Fig. 4. Mag2 has a capped helix dipole that inhibits base excision activity. (A) Close-up view of the DNA interrogating loop. The arrow denotes the direction of the dipole of helix D, with the positive end toward the DNA. The position of Asp56 is marked with a negative sign (−), and the position of the intercalating plug residue, Lys53, is marked with an asterisk (*). (B) Representative εA excision activity for Mag1, Mag2, and Mag2-Asp56Ser mutant. The image shows the electrophoretic separation of the 25 mer εA–DNA substrate (S) from 12 mer product (P) generated from alkaline cleavage of abasic sites produced by the glycosylase. Reaction times in hours are shown at the top. (C) Quantitation of εA activity data, shown as the average of three independent experiments.

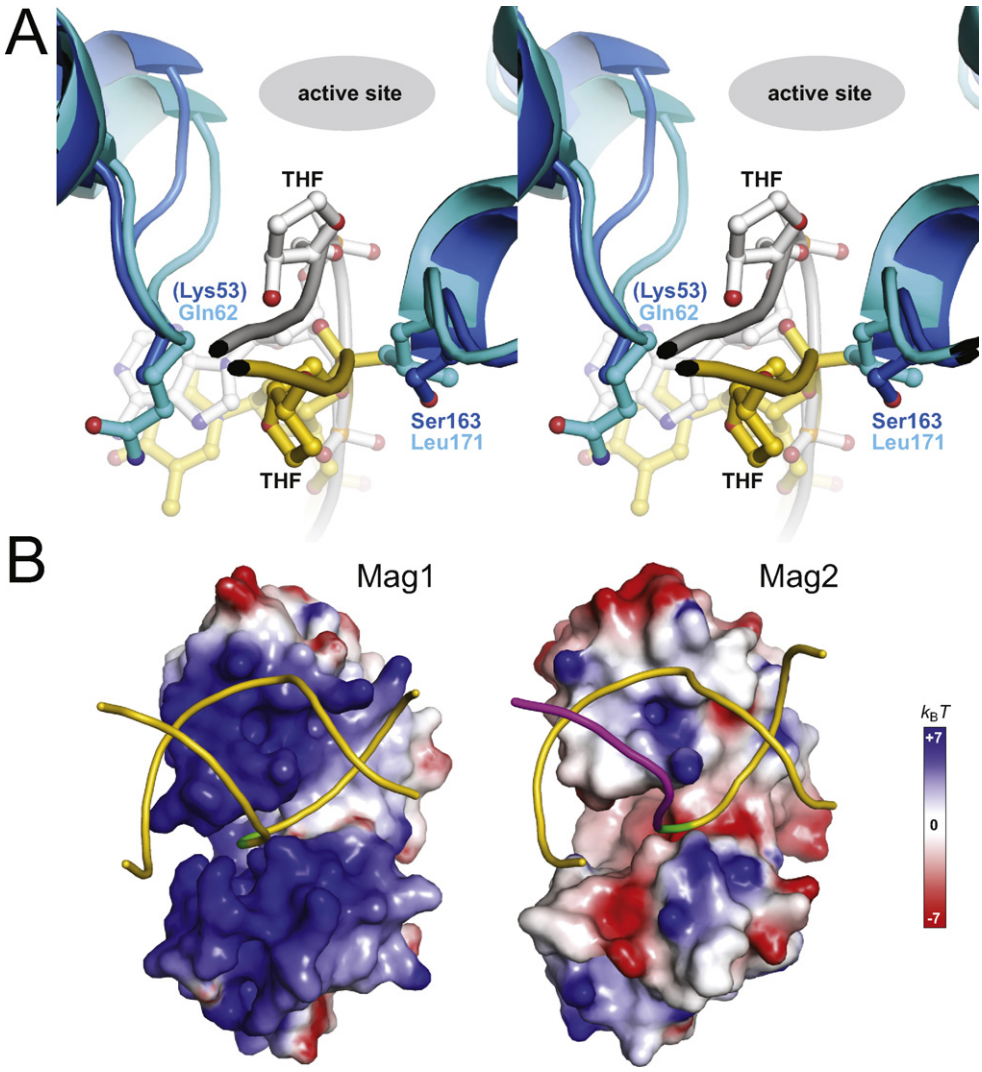

Fig. 5. Additional structural differences between Mag1 and Mag2 that likely impact DNA binding and base flipping. (A) Protein–DNA interactions around the abasic site. The Mag2 complex is colored blue (protein) and gold (DNA), and the Mag1 complex is cyan and silver. The phosphate backbone and main-chain protein atoms are traced with a cartoon. Only the damaged DNA strand is shown for clarity. The active site is at the top of the figure, and the outside of the protein (solvent) is at the bottom. (B) Solvent-accessible surfaces colored according to electrostatic potential (red, negative; blue, positive; −7 to +7 k_BT) calculated using DelPhi [52]. The DNA is colored as in Fig. 2. (For interpretation of the references to color in this figure legend, the reader is referred to the web version of the article.)

Helix D at the base of the intercalating loop normally forms a favorable dipole interaction with the DNA in which its N-terminal end is directed into the minor groove around the lesion (Fig. 4A). In Mag2, this dipole is capped with an aspartate residue (Asp56) at the N-terminal end of helix D, whereas this position is occupied by serine or lysine in Mag1 orthologs and glycine in Mag (Fig. 2D and Supplementary Figure S2). We hypothesized that the neutralized dipole in Mag2 would weaken the interaction between the intercalating CD loop and the DNA, which would consequently impair the protein's ability to stabilize an extrahelical nucleotide. We tested this by substituting Asp56 with serine and measuring εA excision activity. As seen in Fig. 4B and 4C, the Asp56Ser mutation endows Mag2 with the ability to excise εA at levels similar to Mag1. This result strongly suggests that in addition to the direct protein-intercalating residues, a helix dipole in this vicinity of the DNA damage site is important for stabilizing the protein–DNA complex for catalysis.

Further inspection of the structure offers several additional explanations for the disengaged DNA and lack of εA excision activity of Mag2. In Mag1, the backbone of the flipped THF is extruded toward the active site and stabilized by a van der Waals contact from the side chain of Leu171 (Fig. 5A). At this same position in Mag2 is a serine residue (Ser163), which would not provide the steric bulk to divert the backbone in the extruded position. In addition to steric effects, the overall surface charge likely contributes to the disengaged DNA complex in Mag2. Whereas the DNA binding surface of Mag1 is highly positively charged, Mag2 shows patches of negative charge (Fig. 5B). Most notably, the surface of the N/C-terminal domain that normally cradles the DNA 5′ to the lesion is strongly negative in Mag2. Thus, although many of the specific protein–DNA contact points are similar between the two proteins, the overall electrostatic surface landscape may contribute to the instability of the protein–DNA complex.

4. Discussion

4.1. New insight into how glycosylases stabilize the DNA complex

The high sequence and structural similarity between Mag1 and Mag2, and now the availability of both structures bound to THF–DNA offers a unique glimpse into the chemical and physical requirements for base excision activity by the HhH glycosylases,

which include AlkA, TAG, Ogg1, MutY, Endo III, and the 5mC glycosylases DEMETER/ROS1 [1]. Structural and biochemical studies to date have shown that glycosylase residues that intercalate the base stack are critical for interrogating the duplex in search of damage and stabilizing the extrahelical nucleotide and in a variety of protein architectures [1,42,43]. To establish a fully docked enzyme–substrate complex, a side chain plug fills the void created in the duplex from the flipped nucleotide, and a bulky wedge residue stacks against the bases on the opposite strand to stabilize the sharp kink in the duplex. The present work reveals that in addition to the direct steric effects, there exist more subtle, electronic interactions with the duplex that are required for the protein to fully engage the damage, and that in this case can explain the discrepancy in Mag1 and Mag2 activities.

The base excision activity observed in the Mag2 Asp56Ser mutant provides new insight into the ensemble of interactions necessary for the enzyme to fully engage damaged DNA. To our knowledge, this is the most dramatic gain of function for any DNA glycosylase. We previously showed that Mag1 contains an inhibitory histidine residue (His64) that resides on the plug/wedge loop and that interacts directly with nucleobases adjacent to the lesion. Removal of this interaction through a His64Ser substitution increased Mag1 εA activity 4-fold [10]. We speculated that the inhibition by His64 could be due to a perturbation in enzyme–substrate complex or to a slowed search for damage from a greater number of protein–DNA interactions. In contrast, the Mag2 Asp56 interaction is more subtle and the inhibition of activity is most likely due to a weakened dipole–phosphate interaction or a greater electrostatic repulsion between aspartate and the phosphate backbone, either of which would lead to a sub-optimal interaction between helix D and the minor groove and an altered position of the intercalating loop that harbors the plug/wedge residues. Indeed, the Lys53 plug in Mag2 is disordered, even though its C_α is aligned with the gap in the DNA at the THF site. We note that all three helix-coil-helix interactions that anchor the protein to the DNA—helices CD, FG, and IJ—typically contain a positive charge at the N-terminal end of the second helix, which would strengthen the dipole interaction with the DNA (Fig. 2). More work will be required to determine if interactions involving helix D in particular play a more direct role in enzyme–substrate engagement aside from merely stabilizing the intercalation loop.

The un-flipped THF in Mag2 is reminiscent of TAG in complex with THF–DNA and free 3mA, which showed static disorder of the abasic site that interconverted between partially flipped and un-flipped conformations. Contrary to the Mag2–DNA complex, however, the DNA strand upstream of the abasic site in the TAG structure was highly ordered (Figure S3). This implied that the stabilized DNA is a requisite for TAG activity, and it was speculated that the protein uses significant binding energy from protein–DNA interactions within the 3mA binding pocket to aid in breakage of the relatively weak 3mA *N*-glycosidic bond through steric strain [44]. Mag2, on the other hand, is apparently missing those key elements to help stabilize the DNA upstream of the lesion, precluding glycosylase activity. The structural basis for the disordered 5′ strand in Mag2 (and the highly ordered 5′ strand in TAG and Mag1) is unclear given the lack of protein contacts. Nonetheless, the similarity in positions of the un-flipped THF in TAG and Mag2 suggest that the structure of the upstream DNA is not directly coupled to the conformation of the abasic site. Furthermore, we speculate that unlike TAG, the nucleobase binding pockets in the Mag enzymes play only a minor role in stabilizing the complex, given the conservation of Mag1 and Mag2 pockets and the growing number of structures with abasic sites rotated toward the pocket even in the absence of damaged base.

4.2. Repair of base damage in S. pombe

Most fungi have a single copy of Mag, with only the *Schizosaccharomyces* clade preserving two paralogous copies. The persistence of the Mag1 and Mag2 proteins in all *Schizosaccharomyces* species suggests that both are functional, consistent with genetic analysis showing Mag1 and Mag2 play a role in *nth1*-mediated BER [26]. The relatively longer evolutionary branch leading to *S. pombe* Mag2 relative to Mag1 suggests that the duplicates might have at least partially subfunctionalized, with Mag1 generally retaining a greater proportion of Mag's ancestral function and, thus, having more functionally in common with *S. cerevisiae* Mag. A potential alternative interpretation to a purely subfunctionalization model is that Mag2 may have gained additional functionality after its duplication in the *Schizosaccharomyces* ancestor and subsequent sequence divergence. Intriguingly, the trajectory of functional divergence between Mag1 and Mag2 after duplication may not be simple. For example, the relatively short terminal branch of Mag2 in *S. japonicus* suggests that this protein might have been more functionally constrained, and may have perhaps maintained a greater proportion of the ancestral function of Mag, than the Mag2 copies found in the three other *Schizosaccharomyces* species. Consequently, we can infer that Mag2's functional divergence from Mag1 occurred over a long period of evolutionary time.

Mag2's divergence may be indicative of a specialized DNA repair program in *S. pombe* compared to other fungal species and bacteria. Indeed, BER in *S. pombe* exhibits distinct features despite the conservation in protein components with *E. coli*. Firstly, the organism possesses only one bifunctional DNA glycosylase (Nth1) and no functional homologs of Fpg or NEIL enzymes [45,46]. Secondly, it was recently reported that unlike other organisms, repair of AP sites in *S. pombe* can be completed by a polynucleotide kinase Tdp1, independent of AP endonuclease (apn2) [46]. Studies in *S. pombe* have also revealed that sensitivity to alkylating agents do not rely solely on the glycosylase, suggesting crosstalk between various repair pathways [24–26]. Our evolutionary analysis leaves open the possibility that Mag2 does indeed have a function that has not yet been identified. The Mag2–DNA structure argues against a glycolytic role, but it may be that we have yet to uncover the true substrate for Mag2. It is also possible that the *in vivo* activity is modulated by a particular binding partner, as evident in other glycosylases [47–50]. Although the true role of Mag2 remains to be determined, the work presented here highlights some key, previously hidden, DNA interactions necessary for stabilizing the glycosylase–DNA complex.

Conflict of interest

The authors declare that they have no conflict of interest.

Author contribution

B.F.E. oversaw the project; S.A. planned and executed the crystallographic experiments and oversaw the biochemical experiments; M.C.C. generated mutants and performed activity assays; K.M. and A.R. planned and executed the evolutionary analysis; all authors contributed to writing the manuscript.

Acknowledgments

This work was funded by the National Institutes of Health (R01 ES019625). The authors thank the LS-CAT beamline staff at the Advanced Photon Source (Argonne National Laboratory). Use of the APS was supported by the U.S. Department of Energy, Office of Science, Office of Basic Energy Sciences, under Contract No.

DE-AC02-06CH11357. Use of the LS-CAT Sector 21 was supported by the Michigan Economic Development Corporation and the Michigan Technology Tri-Corridor (Grant 085P1000817). Support from the Vanderbilt University Beckman Scholars Program to M.C.C. is gratefully acknowledged.

Appendix A. Supplementary data

Supplementary data associated with this article can be found, in the online version, at http://dx.doi.org/10.1016/j.dnarep.2012.12.001.

References

[1] S.C. Brooks, S. Adhikary, E.H. Rubinson, B.F. Eichman, Recent advances in the structural mechanisms of DNA glycosylases, Biochim. Biophys. Acta 1834 (2013) 247–271.
[2] Y.L. Jiang, K. Kwon, J.T. Stivers, Turning on uracil-DNA glycosylase using a pyrene nucleotide switch, J. Biol. Chem. 276 (2001) 42347–42354.
[3] A.C. Vallur, J.A. Feller, C.W. Abner, R.K. Tran, L.B. Bloom, Effects of hydrogen bonding within a damaged base pair on the activity of wild type and DNA-intercalating mutants of human alkyladenine DNA glycosylase, J. Biol. Chem. 277 (2002) 31673–31678.
[4] B.F. Eichman, E.J. O'Rourke, J.P. Radicella, T. Ellenberger, Crystal structures of 3-methyladenine DNA glycosylase MagIII and the recognition of alkylated bases, EMBO J. 22 (2003) 4898–4909.
[5] A.L. Livingston, S. Kundu, M. Henderson Pozzi, D.W. Anderson, S.S. David, Insight into the roles of tyrosine 82 and glycine 253 in the Escherichia coli adenine glycosylase MutY, Biochemistry 44 (2005) 14179–14190.
[6] A. Maiti, M.T. Morgan, A.C. Drohat, Role of two strictly conserved residues in nucleotide flipping and N-glycosylic bond cleavage by human thymine DNA glycosylase, J. Biol. Chem. 284 (2009) 36680–36688.
[7] A. Banerjee, W.L. Santos, G.L. Verdine, Structure of a DNA glycosylase searching for lesions, Science 311 (2006) 1153–1157.
[8] Y. Qi, M.C. Spong, K. Nam, A. Banerjee, S. Jiralerspong, M. Karplus, G.L. Verdine, Encounter and extrusion of an intrahelical lesion by a DNA repair enzyme, Nature 462 (2009) 762–766.
[9] B.R. Bowman, S. Lee, S. Wang, G.L. Verdine, Structure of *Escherichia coli* AlkA in complex with undamaged DNA, J. Biol. Chem. 285 (2010) 35783–35791.
[10] S. Adhikary, B.F. Eichman, Analysis of substrate specificity of *Schizosaccharomyces pombe* Mag1 alkylpurine DNA glycosylase, EMBO Rep. 12 (2011) 1286–1292.
[11] P.E. Gallagher, T.P. Brent, Partial purification and characterization of 3-methyladenine-DNA glycosylase from human placenta, Biochemistry 21 (1982) 6404–6409.
[12] B. Singer, A. Antoccia, A.K. Basu, M.K. Dosanjh, H. Fraenkel-Conrat, P.E. Gallagher, J.T. Kusmierek, Z.H. Qiu, B. Rydberg, Both purified human 1,N6-ethenoadenine-binding protein and purified human 3-methyladenine-DNA glycosylase act on 1,N6-ethenoadenine and 3-methyladenine, Proc. Natl. Acad. Sci. U.S.A. 89 (1992) 9386–9390.
[13] T.R. O'Connor, Purification and characterization of human 3-methyladenine-DNA glycosylase, Nucleic Acids Res. 21 (1993) 5561–5569.
[14] B.P. Engelward, G. Weeda, M.D. Wyatt, J.L. Broekhof, J. de Wit, I. Donker, J.M. Allan, B. Gold, J.H. Hoeijmakers, L.D. Samson, Base excision repair deficient mice lacking the Aag alkyladenine DNA glycosylase, Proc. Natl. Acad. Sci. U.S.A. 94 (1997) 13087–13092.
[15] B. Hang, B. Singer, G.P. Margison, R.H. Elder, Targeted deletion of alkylpurine–DNA–N-glycosylase in mice eliminates repair of 1,N6-ethenoadenine and hypoxanthine but not of 3,N4-ethenocytosine or 8-oxoguanine, Proc. Natl. Acad. Sci. U.S.A. 94 (1997) 12869–12874.
[16] P.J. O'Brien, T. Ellenberger, Dissecting the broad substrate specificity of human 3-methyladenine-DNA glycosylase, J. Biol. Chem. 279 (2004) 9750–9757.
[17] L. Samson, J. Cairns, A new pathway for DNA repair in *Escherichia coli*, Nature 267 (1977) 281–283.
[18] J. Chen, B. Derfler, L. Samson, *Saccharomyces cerevisiae* 3-methyladenine DNA glycosylase has homology to the AlkA glycosylase of *E. coli* and is induced in response to DNA alkylation damage, EMBO J. 9 (1990) 4569–4575.
[19] J. Chen, L. Samson, Induction of *S. cerevisiae* MAG 3-methyladenine DNA glycosylase transcript levels in response to DNA damage, Nucleic Acids Res. 19 (1991) 6427–6432.
[20] M. Saparbaev, K. Kleibl, J. Laval, *Escherichia coli*, *Saccharomyces cerevisiae*, rat and human 3-methyladenine DNA glycosylases repair 1,N^6-ethenoadenine when present in DNA, Nucleic Acids Res. 23 (1995) 3750–3755.
[21] G.M. Lingaraju, M. Kartalou, L.B. Meira, L.D. Samson, Substrate specificity and sequence-dependent activity of the *Saccharomyces cerevisiae* 3-methyladenine DNA glycosylase (Mag), DNA repair 7 (2008) 970–982.
[22] A. Memisoglu, L. Samson, Base excision repair in yeast and mammals, Mutat. Res. 451 (2000) 39–51.
[23] A. Memisoglu, L. Samson, Cloning and characterization of a cDNA encoding a 3-methyladenine DNA glycosylase from the fission yeast *Schizosaccharomyces pombe*, Gene 177 (1996) 229–235.
[24] A. Memisoglu, L. Samson, Contribution of base excision repair, nucleotide excision repair, and DNA recombination to alkylation resistance of the fission yeast *Schizosaccharomyces pombe*, J. Bacteriol. 182 (2000) 2104–2112.
[25] I. Alseth, F. Osman, H. Korvald, I. Tsaneva, M.C. Whitby, E. Seeberg, M. Bjoras, Biochemical characterization and DNA repair pathway interactions of Mag1-mediated base excision repair in *Schizosaccharomyces pombe*, Nucleic Acids Res. 33 (2005) 1123–1131.
[26] K. Kanamitsu, H. Tanihigashi, Y. Tanita, S. Inatani, S. Ikeda, Involvement of 3-methyladenine DNA glycosylases Mag1p and Mag2p in base excision repair of methyl methanesulfonate-damaged DNA in the fission yeast *Schizosaccharomyces pombe*, Genes Genet. Syst. 82 (2007) 489–494.
[27] N. Rhind, Z. Chen, M. Yassour, D.A. Thompson, B.J. Haas, N. Habib, I. Wapinski, S. Roy, M.F. Lin, D.I. Heiman, S.K. Young, K. Furuya, Y. Guo, A. Pidoux, H.M. Chen, B. Robbertse, J.M. Goldberg, K. Aoki, E.H. Bayne, A.M. Berlin, C.A. Desjardins, E. Dobbs, L. Dukaj, L. Fan, M.G. FitzGerald, C. French, S. Gujja, K. Hansen, D. Keifenheim, J.Z. Levin, R.A. Mosher, C.A. Muller, J. Pfiffner, M. Priest, C. Russ, A. Smialowska, P. Swoboda, S.M. Sykes, M. Vaughn, S. Vengrova, R. Yoder, Q. Zeng, R. Allshire, D. Baulcombe, B.W. Birren, W. Brown, K. Ekwall, M. Kellis, J. Leatherwood, H. Levin, H. Margalit, R. Martienssen, C.A. Nieduszynski, J.W. Spatafora, N. Friedman, J.Z. Dalgaard, P. Baumann, H. Niki, A. Regev, C. Nusbaum, Comparative functional genomics of the fission yeasts, Science 332 (2011) 930–936.
[28] J.C. Slot, A. Rokas, Horizontal transfer of a large and highly toxic secondary metabolic gene cluster between fungi, Curr. Biol. 21 (2011) 134–139.
[29] K. Katoh, H. Toh, Recent developments in the MAFFT multiple sequence alignment program, Brief. Bioinform. 9 (2008) 286–298.
[30] A. Stamatakis, RAxML-VI-HPC: maximum likelihood-based phylogenetic analyses with thousands of taxa and mixed models, Bioinformatics 22 (2006) 2688–2690.
[31] Z. Otwinowski, W. Minor, Processing of X-ray diffraction data collected in oscillation mode, Methods Enzymol. 276 (1997) 307–326.
[32] A.T. Brunger, P.D. Adams, G.M. Clore, W.L. DeLano, P. Gros, R.W. Grosse-Kunstleve, J.S. Jiang, J. Kuszewski, M. Nilges, N.S. Pannu, R.J. Read, L.M. Rice, T. Simonson, G.L. Warren, Crystallography & NMR system: a new software suite for macromolecular structure determination, Acta Crystallogr. D: Biol. Crystallogr. 54 (Pt 5) (1998) 905–921.
[33] P. Emsley, K. Cowtan, Coot: model-building tools for molecular graphics, Acta Crystallogr. D: Biol. Crystallogr. 60 (2004) 2126–2132.
[34] P.D. Adams, R.W. Grosse-Kunstleve, L.W. Hung, T.R. Ioerger, A.J. McCoy, N.W. Moriarty, R.J. Read, J.C. Sacchettini, N.K. Sauter, T.C. Terwilliger, PHENIX: building new software for automated crystallographic structure determination, Acta Crystallogr. D: Biol. Crystallogr. 58 (2002) 1948–1954.
[35] R.A. Laskowski, J.A. Rullmannn, M.W. MacArthur, R. Kaptein, J.M. Thornton, AQUA and PROCHECK-NMR: programs for checking the quality of protein structures solved by NMR, J. Biomol. NMR 8 (1996) 477–486.
[36] R. Lavery, M. Moakher, J.H. Maddocks, D. Petkeviciute, K. Zakrzewska, Conformational analysis of nucleic acids revisited: Curves+, Nucleic Acids Res. 37 (2009) 5917–5929.
[37] K. Pereira de Jesus, L. Serre, C. Zelwer, B. Castaing, Structural insights into abasic site for Fpg specific binding and catalysis: comparative high-resolution crystallographic studies of Fpg bound to various models of abasic site analogues-containing DNA, Nucleic Acids Res. 33 (2005) 5936–5944.
[38] D.P. Norman, S.D. Bruner, G.L. Verdine, Coupling of substrate recognition and catalysis by a human base-excision DNA repair protein, J. Am. Chem. Soc. 123 (2001) 359–360.
[39] K. Imamura, S.S. Wallace, S. Doublie, Structural characterization of a viral NEIL1 ortholog unliganded and bound to abasic site-containing DNA, J. Biol. Chem. 284 (2009) 26174–26183.
[40] J. Tchou, M.L. Michaels, J.H. Miller, A.P. Grollman, Function of the zinc finger in *Escherichia coli* Fpg protein, J. Biol. Chem. 268 (1993) 26738–26744.
[41] B. Castaing, J.L. Fourrey, N. Hervouet, M. Thomas, S. Boiteux, C. Zelwer, AP site structural determinants for Fpg specific recognition, Nucleic Acids Res. 27 (1999) 608–615.
[42] J.T. Stivers, Site-specific DNA damage recognition by enzyme-induced base flipping, Prog. Nucleic Acid Res. Mol. Biol. 77 (2004) 37–65.
[43] J.T. Stivers, Extrahelical damaged base recognition by DNA glycosylase enzymes, Chemistry 14 (2008) 786–793.
[44] A.H. Metz, T. Hollis, B.F. Eichman, DNA damage recognition and repair by 3-methyladenine DNA glycosylase I (TAG), EMBO J. 26 (2007) 2411–2420.
[45] K. Kanamitsu, S. Ikeda, Early steps in the DNA base excision repair pathway of a fission yeast *Schizosaccharomyces pombe*, J. Nucleic Acids 2010 (2010).
[46] L. Nilsen, R.J. Forstrom, M. Bjoras, I. Alseth, AP endonuclease independent repair of abasic sites in *Schizosaccharomyces pombe*, Nucleic Acids Res. 40 (2012) 2000–2009.
[47] A. Campalans, S. Marsin, Y. Nakabeppu, T.R. O'Connor, S. Boiteux, J.P. Radicella, XRCC1 interactions with multiple DNA glycosylases: a model for its recruitment to base excision repair, DNA Repair 4 (2005) 826–835.
[48] J.T. Mutamba, D. Svilar, S. Prasongtanakij, X.H. Wang, Y.C. Lin, P.C. Dedon, R.W. Sobol, B.P. Engelward, XRCC1 and base excision repair balance in response to nitric oxide, DNA Repair 10 (2011) 1282–1293.
[49] M.R. Baldwin, P.J. O'Brien, Human AP endonuclease 1 stimulates multiple-turnover base excision by alkyladenine DNA glycosylase, Biochemistry 48 (2009) 6022–6033.
[50] M.E. Fitzgerald, A.C. Drohat, Coordinating the initial steps of base excision repair. Apurinic/apyrimidinic endonuclease 1 actively stimulates thymine DNA

glycosylase by disrupting the product complex, J. Biol. Chem. 283 (2008) 32680–32690.
[51] N. Guex, M.C. Peitsch, SWISS-MODEL and the Swiss-PdbViewer: an environment for comparative protein modeling, Electrophoresis 18 (1997) 2714–2723.
[52] W. Rocchia, S. Sridharan, A. Nicholls, E. Alexov, A. Chiabrera, B. Honig, Rapid grid-based construction of the molecular surface and the use of induced surface charge to calculate reaction field energies: applications to the molecular systems and geometric objects, J. Comput. Chem. 23 (2002) 128–137.